

# PART III ESSAY: PATTERN FORMATION IN THE PLANE

Christopher Taylor, Trinity College

## Contents

<b>1</b>	<b>Introduction</b>	<b>2</b>
<b>2</b>	<b>Bifurcation Theory for Symmetric Systems</b>	<b>3</b>
2.1	Equivariance . . . . .	4
2.2	The equivariant branching lemma . . . . .	6
2.3	Bifurcations in a box . . . . .	9
<b>3</b>	<b>Lattice Patterns</b>	<b>12</b>
3.1	Bifurcations on a lattice . . . . .	12
3.2	Steady bifurcation on a square lattice . . . . .	14
3.3	Steady bifurcation on a hexagonal lattice . . . . .	18
3.4	Pseudoscalar patterns . . . . .	21
<b>4</b>	<b>Hallucination Patterns in the Visual Cortex</b>	<b>22</b>
4.1	The human retino-cortical map . . . . .	23
4.2	Modelling V1 . . . . .	24
4.3	Linearization . . . . .	26
4.4	Restriction to a lattice . . . . .	29
4.5	Visual hallucinations . . . . .	30

## 1 Introduction

Patterns appear so frequently in the natural world that it is easy to forget what is so remarkable about them. We would expect that undirected forces acting on a system would produce nothing more than a mess, and so it is surprising to see so many regular patterns cropping up in many different contexts—from convection patterns in a heated fluid to animal markings to the whorls on a human fingerprint.

It is easy to pick out a pattern by eye—we just imagine some structure with a degree of regularity to it, typically periodicity in space, at least at a local level. Mathematically we are concerned with spatially extended structures with some symmetry properties; perhaps reflection symmetry or local invariance under a rotation.

We model a pattern as a scalar function  $u(x, y, t)$  on the plane which satisfies some partial differential equation, with the understanding that the value of this function represents some quantity of interest in the system that we are studying—for example it could represent vertical fluid velocity if we are studying a convection experiment, or concentration of a product in a reaction-diffusion system. Because we expect patterns to be periodic, we expand  $u$  as a series of two-dimensional Fourier modes, each of which has a time-dependent amplitude. We can then use the specifics of the system we are studying to deduce evolution equations for those amplitudes, which we call amplitude equations. This is useful, but has the drawback that we must start our analysis from the beginning every time we want to study a new system.

We can take an alternative approach by noticing that the most common naturally-occurring patterns are stripes, squares and hexagons. These patterns occur frequently in different physical contexts but share very similar properties—for example the stripes on a zebra's back look remarkably similar to convection rolls, which in turn look similar to ripples on sand dunes. This leads us to speculate that rather than dealing with specific systems, it might be profitable to deduce amplitude equations from the observable features and symmetries of the pattern and its environment.

Because we want to study pattern *formation* we must look at a scenario where a system in which there is no pattern spontaneously changes to display a pattern, usually due to some external forcing. For example, in a convection experiment we might have a shallow tray of fluid in which we keep the temperature of the top layer constant, and can vary the temperature of the bottom layer. At low temperatures we find that there is no pattern—this is the zero state, or pure conduction state, as the fluid is not moving. When we slowly increase the temperature of the bottom layer there comes a point where a pattern of convection rolls emerges. We have shifted from the pure conduction state to a pattern where heat is also transferred via convection, or circulating fluid. Mathematically this means that we need to use bifurcation theory: the theory that describes how smooth changes in the input of a system can produce sudden changes in the output.

More precisely, we want to study bifurcation theory for systems with symmetry. This is in many respects much more interesting, as the potential for more complex bifurcations is far greater. For

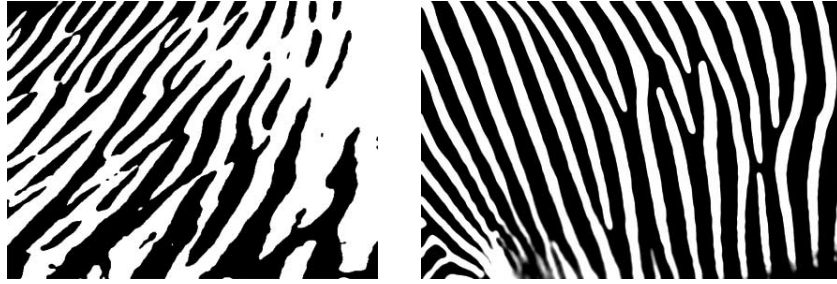


Figure 1: Monochrome images showing ripples in sand dunes on the left, and stripes on a zebra's coat on the right. Note the similarity between the two, particularly in the points where one stripe divides into two.

example, we will always be assuming the existence of a trivial zero state, which corresponds to a fixed point at the origin. Thus the generic bifurcations will be transcritical or pitchfork bifurcations, rather than the saddle-nodes that we would expect if there were no symmetry. It turns out that we can say quite a lot about the fixed points that emerge from a bifurcation just by knowing something about the symmetry group of the problem.

This essay is organised as follows. Section 2 develops ideas in symmetric bifurcation theory and introduces some key ideas and notation before going on to a discussion of the equivariant branching lemma, an important result which tells us about the fixed points that can emerge from a symmetric bifurcation. In Section 3 we apply these ideas to pattern-forming systems, specifically patterns which sit on a lattice, with the extended example of patterns on a square lattice and a brief discussion of pseudoscalar patterns, which display an altered symmetry group. Section 4 discusses a specific example in detail—that of geometric hallucination patterns in the visual cortex.

As regards notation, we will usually use non-bold symbols to denote both scalar and vector quantities, e.g.  $x \in \mathbb{R}^n$ . It will be clear from the context what is meant. We will sometimes use bold symbols to denote a vector when it would be confusing not to do so—for example, when we want to write  $\mathbf{x} = (x, y)$ .

## 2 Bifurcation Theory for Symmetric Systems

In this section we lay out the groundwork for further study of pattern formation, namely a consideration of dynamical systems with symmetry. We first lay out some basic results in group theory and representation theory before going on to develop the theory of bifurcations in symmetric systems in more detail, which will prepare us for a statement and proof of the equivariant branching lemma, an important result which relates the symmetry of steady solutions to the symmetry of the pattern-forming system in which they are seen.

### Preliminary theory

We would like to consider bifurcations in systems with some symmetry properties. In general, our system is specified by a system of equations

$$\dot{x} = f(x, \mu) \tag{1}$$

where  $x$  is a vector describing a position in phase space, and  $\mu$  is a real bifurcation parameter. Throughout this section we will take  $x \in \mathbb{R}^n$ . This system has a steady bifurcation if we have a fixed point  $x_0$  such that the linearisation  $Df|_{(x_0, \mu)}$  has a real eigenvalue passing through zero at the bifurcation point,  $\mu = \mu_c$ . By choosing our origins appropriately we can always ensure that the bifurcation occurs at  $x = 0$  and  $\mu = 0$ .

Our symmetry is described by some symmetry group  $\Gamma$ , with elements  $\gamma$ . We will assume that  $\Gamma$  is a finite group or a compact Lie group—there has been some progress in describing the bifurcations of a system with a non-compact symmetry group, but the problem is much more difficult. The action of this group on  $\mathbb{R}^n$  is via some representation of the group, i.e. a homomorphism from the group to the set of  $n \times n$  real matrices

$$\begin{aligned} \theta : \Gamma &\rightarrow GL(n, \mathbb{R}) \\ \gamma &\mapsto \theta(\gamma). \end{aligned}$$

We will use a condensed notation, where  $\gamma x$  is shorthand for  $\theta(\gamma)x$ , the action of the group element  $\gamma$  on the vector  $x$ .

A subspace  $V$  of phase space  $\mathbb{R}^n$  is said to be  $\Gamma$ -invariant under some representation if  $\Gamma$  maps  $V$  back into itself, i.e. if

$$\gamma v \in V \quad \forall v \in V, \forall \gamma \in \Gamma.$$

For example, if  $SO(2)$  acts on  $\mathbb{R}^3$  by rotating around the  $z$ -axis then both the  $z$ -axis and the  $(x, y)$  plane are invariant subspaces. It is obvious that both the whole of  $\mathbb{R}^n$  and the origin  $\{0\}$  are always invariant—these are the trivial invariant subspaces.

We say that a group acting via some representation acts *irreducibly* on  $\mathbb{R}^n$  if there are no non-trivial invariant subspaces. We say that a group acts *absolutely irreducibly* if the only matrices that commute with all elements of the group are multiples of the identity matrix. As we might expect, an absolutely irreducible representation is also irreducible. For our purposes we need to know that absolutely irreducible representations of symmetry groups give rise to steady bifurcations in systems that have that symmetry. Representations that are irreducible but not absolutely irreducible give rise to oscillatory bifurcations, but we will not touch on those in this essay.

## 2.1 Equivariance

We begin by considering a dynamical system with a bifurcation

$$\dot{x} = f(x, \mu) \tag{2}$$

with  $x \in \mathbb{R}^n$  and bifurcation parameter  $\mu \in \mathbb{R}$ . We make a change of variables so that the bifurcation occurs at  $\mu = 0$ . We want to consider systems with symmetry, so we assume that the equations are invariant under the action of some symmetry group  $\Gamma$  with elements  $\gamma$ . Thus whenever  $x(t)$  is a solution of (2) we would like  $\gamma x(t)$  to be a solution as well. Consideration of the form of the equations then leads us to an *equivariance condition*

$$\gamma f(x, \mu) = f(\gamma x, \mu) \quad \forall \gamma \in \Gamma. \quad (3)$$

Equivariance is the requirement that the left and right sides of (2) transform in such a way as to preserve the form of the equations. From this seemingly innocuous condition we can nevertheless gain much information. For example, assume we have an equilibrium point  $x$  which satisfies  $f(x, \mu) = 0$ . Then

$$f(\gamma x, \mu) = \gamma f(x, \mu) = 0$$

so  $\gamma x$  is also an equilibrium point. We can also show that these additional fixed points have the same stability properties as the original point. Differentiating the equivariance condition (3) gives

$$\gamma Df|_{(x, \mu)} = Df|_{(\gamma x, \mu)} \gamma \quad \forall \gamma \in \Gamma. \quad (4)$$

If the Jacobian has an eigenvector  $v$  with eigenvalue  $\lambda$ , so that

$$Df|_{(x, \mu)} v = \lambda v.$$

then using (4), we see that

$$Df|_{(\gamma x, \mu)} \gamma v = \gamma Df|_{(x, \mu)} v = \lambda \gamma v$$

and so  $\gamma v$  is an eigenvector of  $Df|_{(\gamma x, \mu)}$  with the same eigenvalue. Thus for every fixed point  $x$  there is a fixed point  $\gamma x$ , and the linearisation near that fixed point has the same eigenvalues, so the fixed point  $\gamma x$  has the same stability properties.

### Isotropy subgroups

The symmetry of a stationary solution  $x$  is given by its *isotropy subgroup*  $\Sigma_x \subset \Gamma$  defined by,

$$\Sigma_x = \{\sigma \in \Gamma : \sigma x = x\} \quad (5)$$

We say that two points  $x$  and  $y$  are on the same group orbit if  $y = \gamma x$  for some  $\gamma \in \Gamma$ . We can then note that points on the same orbit of  $x$  have conjugate isotropy subgroups,

$$\Sigma_{\gamma x} = \gamma \Sigma_x \gamma^{-1}.$$

To see this, notice that  $\gamma \sigma \gamma^{-1} \gamma x = \gamma \sigma x = \gamma x$ , and so the elements of  $\gamma \Sigma_x \gamma^{-1}$  fix all points of the form  $\gamma x$ .

The *conjugacy class* of an isotropy subgroup  $\Sigma_x$  is the set of all isotropy subgroups conjugate to it. If we say that two point  $x, y$  are on the same *group orbit*, we mean that they have conjugate isotropy subgroups.

### Fixed-point subspaces

We define the *fixed-point subspace*  $\text{Fix}(\Sigma)$  of a subgroup  $\Sigma \subset \Gamma$  to be the set of points in  $V$  which are fixed by the action of  $\Sigma$ :

$$\text{Fix}(\Sigma) = \{x \in V : \sigma x = x \quad \forall \sigma \in \Sigma\}. \quad (6)$$

$\text{Fix}(\Sigma)$  is non-empty, since  $\sigma 0 = 0$ . Also, because  $\sigma$  is a linear map  $\text{Fix}(\Sigma)$  is closed under addition and scalar multiplication. Hence  $\text{Fix}(\Sigma)$  is indeed a subspace of  $V$ .

We can also see that  $\text{Fix}(\Sigma)$  is flow-invariant, i.e. elements in the subspace stay in the subspace when we evolve the system. We notice that

$$\sigma f(x, \mu) = f(\sigma x, \mu) = f(x, \mu) \quad \forall x \in \text{Fix}(\Sigma),$$

and thus  $f(\text{Fix}(\Sigma), \mu) \subseteq \text{Fix}(\Sigma, \mu)$ . If we are looking for a solution to our system of equations which has a symmetry given by the isotropy subgroup  $\Sigma_x$  we can just restrict  $f$  to  $\text{Fix}(\Sigma)$  and solve the equations there. This is especially useful when  $\text{Fix}(\Sigma)$  is one-dimensional, because the equations become much easier to analyse.

To simplify our calculations we want to consider systems where the symmetry group doesn't have any redundancy—i.e. the only point fixed by the entire group is the origin. We don't need to consider directions which are fixed by the entire group, and so we want  $\text{Fix}(\Gamma) = \{0\}$ . This condition holds if we use a non-trivial irreducible representation of the group  $\Gamma$ .

With this condition there is always a trivial solution to our system of equations, namely the steady solution at the origin. We have  $\gamma f(0, \mu) = f(0, \mu)$  and thus  $f(0, \mu) \in \text{Fix}(\Gamma)$ . But only the origin is fixed by the whole of  $\Gamma$ , and so  $f(0, \mu) = 0$ .

Another benefit of this condition is that any non-trivial isotropy subgroup  $\Sigma \subset \Gamma$  will satisfy  $\dim \text{Fix}(\Sigma) \geq 1$ .

An isotropy subgroup which has  $\dim \text{Fix}(\Sigma) = 1$  is said to be *axial*, by analogy with a rotation in three dimensions which fixes a one-dimensional axis. Axial isotropy subgroups are important because we can restrict our bifurcation problem to their fixed point subspaces, and it turns out that the problem is easy to analyse there.

## 2.2 The equivariant branching lemma

The equivariant branching lemma is an important result which makes predictions about the symmetry of solutions which emerge at a steady bifurcation, based on the symmetry of the bifurcation problem. Loosely speaking it says that if we have a  $\Gamma$ -equivariant bifurcation problem with a steady bifurcation at the origin, and an axial isotropy subgroup  $\Sigma$ , then we will see bifurcating branches that have the same symmetry group  $\Sigma$ .

As a toy model consider a one-dimensional system which has  $\mathbb{Z}_2$  symmetry, so that  $-x$  has the same evolution equation as  $x$ . We write this

$$\dot{x} = f(x, \mu).$$

Assume that  $\mathbb{Z}_2$  doesn't act trivially, i.e. it doesn't act via the identity representation. Then by our equivariance condition we must have  $f(-x, \mu) = -f(x, \mu)$ , i.e.  $f$  is odd, and so we expand in a Taylor series in  $x$ :

$$f(x, \mu) = \mu x + ax^3 + \dots$$

The coefficient of  $x$  must be  $\mu$ , to give a bifurcation at  $\mu = 0$ . We see immediately that the generic bifurcation at the origin will be a pitchfork, rather than the transcritical bifurcation that we might expect if there were no symmetry in the equations. Indeed, a pitchfork bifurcation has  $\mathbb{Z}_2$  symmetry, as there are identical bifurcating branches above and below the  $\mu$ -axis.

### Statement and proof

Recall that if  $\Gamma$  acts absolutely irreducibly then the only matrices commuting with all  $\gamma \in \Gamma$  are scalar multiples of the identity. If we differentiate the equivariance condition (3) and set  $x = 0$  then we find that

$$Df|_{(0,\mu)}\gamma = \gamma Df|_{(0,\mu)} \quad \forall \gamma \in \Gamma.$$

Thus the Jacobian evaluated at the origin must be a scalar multiple of the identity:  $Df|_{(0,\mu)} = c(\mu)I$  for some function  $c(\mu)$  satisfying  $c(0) = 0$ . Thus all eigenvalues pass through 0 at the origin, so the bifurcation is steady.

We also require that the eigenvalues pass through the origin with non-zero 'speed' to give a non-degenerate bifurcation. Thus we want  $\partial_\mu Df|_{(0,0)}v \neq 0$  for any nonzero  $v \in \text{Fix}(\Sigma)$ . This corresponds to

$$c'(0) \neq 0 \tag{7}$$

which we want to hold simultaneously for all isotropy subgroups  $\Sigma \subset \Gamma$ . This condition preserves genericity, as a function  $c(\mu)$  with  $c'(\mu) = 0$  can be perturbed to give a different bifurcation. For example,  $c(\mu) = \mu^3$  can be perturbed to  $c(\mu) = \mu^3 - \epsilon\mu$ , but that crosses the axis three times rather than just once. We can now state the equivariant branching lemma:

**Theorem 1 (The equivariant branching lemma).** *Let  $\Gamma$  be a finite group or a compact Lie group which acts absolutely irreducibly on a real vector space  $V$ , and let*

$$\dot{x} = f(x, \mu)$$

*be a  $\Gamma$ -equivariant bifurcation problem. This implies that  $f(0, \mu) = 0$  and*

$$Df|_{(0,\mu)} = c(\mu)I, \quad c(0) = 0.$$

*If  $c'(\mu) \neq 0$  and  $\Sigma$  is an axial isotropy subgroup, then there exists a unique branch of solutions to  $f(x, \mu) = 0$  emanating from the origin, and the symmetry of the solutions is  $\Sigma$ .*

*Proof.* Since  $\Sigma$  is axial, we have  $\dim \text{Fix}(\Sigma) = 1$ , so let  $v$  be a nonzero vector in  $\text{Fix}(\Sigma)$ , which must span the subspace. We know that  $\text{Fix}(\Sigma)$  is flow-invariant, so the evolution of  $v$  is a scalar multiple of  $v$ :

$$\dot{av} = f(av, \mu) = g(a, \mu)v.$$

Because  $f(0, \mu) = 0$  we must also have  $g(0, \mu) = 0$ , and so we can rewrite:

$$\dot{a} = g(a, \mu) = ah(a, \mu).$$

The linearisation is  $\dot{a} = ah(0, \mu)$ , and so we must have  $h(0, \mu) = c(\mu)$ , so that  $h(0, 0) = 0$  and  $\partial_\mu h(0, 0) \neq 0$ . With these conditions we can apply the Implicit Function Theorem to deduce that there is a unique  $\mu(a)$  such that  $\mu(0) = 0$  and  $h(a, \mu(a)) \equiv 0$ . Thus  $f(av, \mu(a)) = 0$  and we have our smooth solution branch.

It remains to show that the isotropy subgroup of these solutions is  $\Sigma$ . They certainly lie in  $\text{Fix}(\Sigma)$ , and so their isotropy group  $\Sigma_v$  includes  $\Sigma$ . But  $\Sigma$  is an isotropy subgroup itself, and so  $\Sigma_v = \Sigma$ .  $\square$

## Applications

We now explore some simple examples of the equivariant bifurcation lemma in action, in order to get a feel for it before moving on to some more complicated applications.

- (i) Let  $\Gamma = O(2)$  act on  $\mathbb{R}^2$ , and make the identification  $\mathbb{R}^2 \equiv \mathbb{C}$ . The action on  $z \in \mathbb{C}$  is generated by a rotation  $\theta$  and a reflection  $m$ , which act as

$$\theta z = e^{i\theta} z, \quad mz = \bar{z}.$$

The subgroup  $\Sigma = \{1, m\}$  has  $\text{Fix}(\Sigma) = \mathbb{R}$ , and so it is axial. Thus in a generic bifurcation we expect to see solutions with reflectional symmetry.

- (ii) Let  $\Gamma = S_3$  act on  $\mathbb{R}^3$  subject to  $x + y + z = 0$  by permuting the coordinates. Thus  $(12)(x, y, z) = (y, x, z)$  etc. There is a trivial fixed point at the origin, which will lose stability as our bifurcation parameter passes through zero.

The  $S_2$  subgroup given by  $\Sigma = \{e, (12)\}$  has  $\text{Fix}(\Sigma) = \{(x, x, z)\}$ , which is axial, and so in a generic bifurcation we expect to see fixed points with two coordinates equal. The other two isotropy subgroups  $\{e, (13)\}$  and  $\{e, (23)\}$  give a total of three solution branches, each with two coordinates equal.

This can be interpreted as a (very) crude model for speciation, where we have three clusters of organisms and the labels  $x$ ,  $y$  and  $z$  represent, for example, deviation from mean beak length in birds. The condition  $x + y + z = 0$  ensures that the mean remains constant, and  $S_3$ -equivariance reflects that fact that each cluster reacts to the other two clusters in an identical way. The equivariant branching lemma then predicts diversification into two species, with one species outnumbering the other two to one.

### 2.3 Bifurcations in a box

We now explore the bifurcations that can occur in a square box, i.e. a system with symmetry group  $\Gamma = D_4$ . This is a nice application of the equivariant branching lemma, and will turn out to be useful later when we consider pattern-forming systems on a square lattice. Assuming that the bifurcation is steady, all we have to do is work out the isotropy subgroups and see which ones have a one-dimensional fixed-point subspace, and we immediately have the symmetries of the solution branches at the bifurcation.

The group is generated by  $\rho$ , a rotation by  $\pi/2$ , and  $m$ , a reflection in the horizontal axis. The full group has three rotations and four reflections, and its structure is summarised in Table 1.

The representation of  $D_4$  that we use turns out to be important in this case, as there are many representations which act absolutely irreducibly. For example, the parity representation sends all the rotations to 1, and all the reflections to -1. This will give a different generic bifurcation to if we used the identity representation. In experiments only one representation will be ‘chosen’ and it is impossible for us to predict which one it is ahead of time. Fortunately, absolutely irreducible representations come up often, and so our best strategy is to consider each of the irreps and then see which bifurcation best fits the experiment at hand.

For the purposes of this example we will restrict our attention to the natural representation. We will find it easiest to work in complex notation  $z = x + iy$  to begin with, and only later switch to using real equations. The action of the generators of  $D_4$  on  $\mathbb{C}$  is given by

$$\begin{aligned}\rho : z &\rightarrow iz \\ m : z &\rightarrow \bar{z}.\end{aligned}\tag{8}$$

	$e$	$\rho$	$\rho^2$	$\rho^3$	$m$	$m\rho$	$m\rho^2$	$m\rho^3$
$e$	$e$	$\rho$	$\rho^2$	$\rho^3$	$m$	$m\rho$	$m\rho^2$	$m\rho^3$
$\rho$	$\rho$	$\rho^2$	$\rho^3$	$e$	$m\rho^3$	$m$	$m\rho$	$m\rho^2$
$\rho^2$	$\rho^2$	$\rho^3$	$e$	$\rho$	$m\rho^2$	$m\rho^3$	$m$	$m\rho$
$\rho^3$	$\rho^3$	$e$	$\rho$	$\rho^2$	$m\rho$	$m\rho^2$	$m\rho^3$	$m$
$m$	$m$	$m\rho$	$m\rho^2$	$m\rho^3$	$e$	$\rho$	$\rho^2$	$\rho^3$
$m\rho$	$m\rho$	$m\rho^2$	$m\rho^3$	$m$	$\rho^3$	$e$	$\rho$	$\rho^2$
$m\rho^2$	$m\rho^2$	$m\rho^3$	$m$	$m\rho$	$\rho^2$	$\rho^3$	$e$	$\rho$
$m\rho^3$	$m\rho^3$	$m$	$m\rho$	$m\rho^2$	$\rho$	$\rho^2$	$\rho^3$	$e$

Table 1: Group table of  $D_4$ .

We can write the bifurcation problem as

$$\dot{z} = f(z, \bar{z}, \mu) = \mu z + \sum_{p,q} c_{pq} z^p \bar{z}^q$$

where we have expanded  $f$  as a Taylor series. We can then use our equivariance conditions to restrict the form of  $f$ . Under a rotation, a general term  $z^p \bar{z}^q$  must satisfy

$$i z^p \bar{z}^q = i^{p-q} z^p \bar{z}^q$$

and thus we must have  $p - q \equiv 1 \pmod{4}$ . Up to cubic order, the terms of this form are  $z$ ,  $\bar{z}^3$  and  $|z|^2 z$ . We must also have reflection equivariance, which acting on a term  $c z^p \bar{z}^q$  gives

$$\bar{c} \bar{z}^p z^q = c \bar{z}^p z^q,$$

and so the coefficients must be real. Thus up to cubic order our evolution equation takes the form

$$\dot{z} = \mu z - a \bar{z}^3 - b |z|^2 z,$$

which, if we redefine  $a$  and  $b$ , we can write in real notation as

$$\begin{aligned} \dot{x} &= \mu x - ax^3 - by^2 x \\ \dot{y} &= \mu y - ay^3 - bx^2 y. \end{aligned} \tag{9}$$

In fact we could rescale and find that the bifurcation only depends on the relative magnitude of  $a$  and  $b$ , but we will leave the equations in this form for now.

There is a trivial fixed point at the origin, and we also have fixed points at  $x = \pm\sqrt{\mu/a}$ ,  $y = 0$  and at  $x = 0$ ,  $y = \pm\sqrt{\mu/a}$ . If  $a$  is positive then these fixed points only exist in  $\mu > 0$ , and if  $a$  is negative they exist in  $\mu < 0$ . Remembering that the reflection  $m$  is a reflection in the  $y$ -axis, we see that the isotropy subgroup of the first solution is  $\{e, m\}$  and the isotropy subgroup of the second is  $\{e, m\rho^2\}$ . These are reflections in the vertical and horizontal axes respectively.

We get further fixed points for which  $x = y$  or  $x = -y$ , which occur at  $x = \pm\sqrt{\mu/(a+b)}$ , which can occur on either side of the bifurcation depending on the relative magnitudes of  $a$  and  $b$ . The isotropy subgroups of these solutions are  $\{e, m\rho\}$  and  $\{e, m\rho^3\}$ , which are reflections in the diagonal axes.

We can now perform a stability analysis to see which modes are stable for given values of  $a$  and  $b$ . We can calculate the Jacobian  $Df$  from the normal form equations (9), and it turns out to be

$$Df = \begin{pmatrix} \mu - 3ax^2 - by^2 & -2bxy \\ -2bxy & \mu - 3ay^2 - bx^2 \end{pmatrix}.$$

Evaluating this at the origin gives

$$Df = \begin{pmatrix} \mu & 0 \\ 0 & \mu \end{pmatrix}$$

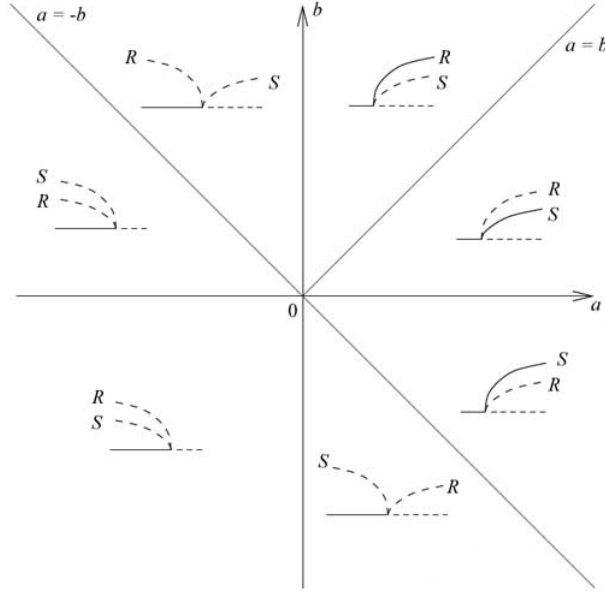


Figure 2: Bifurcation diagrams for a system with  $D_4$  symmetry. Solution branches on the same orbit as  $(x, 0)$  are labelled  $R$ , and solutions on the same orbit as  $(x, x)$  are labelled  $S$ . The vertical axis represents  $|x|$ , and we imagine extending each small bifurcation diagram to full  $D_4$  symmetry.

so that the origin is stable for  $\mu < 0$  and unstable for  $\mu > 0$ . If we evaluate the Jacobian at the solution  $x^2 = \mu/a$ ,  $y = 0$  we get

$$Df = \begin{pmatrix} -2\mu & 0 \\ 0 & \mu(1 - b/a) \end{pmatrix}$$

so in  $\mu > 0$  this solution is stable to perturbations in the  $x$  direction, and it is stable to perturbations in the  $y$  direction if  $a < b$ . The solution with  $y^2 = \mu/a$  has the same stability properties, but the diagonal entries are swapped so that it is always stable to perturbations in the  $y$  direction in  $\mu > 0$ .

Evaluating the Jacobian at the fixed point where  $x = y$  and  $x^2 = \mu/(a + b)$ , we get

$$Df = \begin{pmatrix} -2a\mu/(a + b) & -2b\mu/(a + b) \\ -2b\mu/(a + b) & -2a\mu/(a + b) \end{pmatrix}.$$

We can easily work out the eigenvalues of this matrix, and they turn out to be  $-2\mu$  and  $-2\mu(a - b)/(a + b)$ . The eigenvectors to which these correspond are  $(1, 1)$  and  $(1, -1)$  respectively. Thus in  $\mu > 0$  this fixed point is stable to perturbations in the  $(1, 1)$  direction, and stable to perturbations in the  $(1, -1)$  direction if  $a > b$ . As before, the other diagonal solution has the same stability properties but with the eigenvectors swapped over.

The bifurcation diagrams for the various regions of the  $(a, b)$  plane are shown in Figure 2. We know have a complete description of every solution that is guaranteed to emerge from a steady bifurcation with  $D_4$  symmetry under the natural representation.

### 3 Lattice Patterns

Lattice patterns crop up frequently in nature. The most common patterns are stripes and hexagons, but other patterns such as squares and triangles are also possible. In this section we will apply our techniques from symmetric bifurcation theory to lattice patterns, in order to understand large-scale pattern formation.

#### Lattices

A planar lattice  $\mathcal{L}$  is generated by vectors  $\ell_1, \ell_2 \in \mathbb{R}^2$  and is defined by

$$\mathcal{L} = \{m\ell_1 + n\ell_2 : n, m \in \mathbb{Z}\}. \quad (10)$$

We will also want to make use of the dual lattice  $\mathcal{L}^*$ , which is generated by *wave vectors*  $\mathbf{k}_1, \mathbf{k}_2$  which satisfy  $\mathbf{k}_i \cdot \ell_j = 2\pi\delta_{ij}$ . The dual lattice is defined by

$$\mathcal{L}^* = \{m\mathbf{k}_1 + n\mathbf{k}_2 : n, m \in \mathbb{Z}\}. \quad (11)$$

A *planar lattice pattern* is a function  $u(\mathbf{x}, t)$  of position  $\mathbf{x} \in \mathbb{R}^2$  and time  $t$  which is periodic on the lattice. That is,

$$u(\mathbf{x} + \ell, t) = u(\mathbf{x}, t) \quad \forall \ell \in \mathcal{L}.$$

Thus we can express the pattern as a sum of Fourier modes on the dual lattice,

$$u(\mathbf{x}, t) = \sum_{\mathbf{k} \in \mathcal{L}^*} z_{\mathbf{k}}(t)e^{i\mathbf{k} \cdot \mathbf{x}} + \bar{z}_{\mathbf{k}}(t)e^{-i\mathbf{k} \cdot \mathbf{x}}.$$

The most common physical lattices have  $|\mathbf{k}_1| = |\mathbf{k}_2|$ , which are the square, rhombic and hexagonal lattices.

#### 3.1 Bifurcations on a lattice

Pattern-forming systems are governed by a partial differential equation of the form

$$\frac{\partial u(\mathbf{x}, t)}{\partial t} = f(u(\mathbf{x}, t), \mu) \quad (12)$$

where  $f$  is a nonlinear smooth operator and  $\mu$  is a bifurcation parameter. We interpret the solution  $u(\mathbf{x}, t)$  as some property of a physical system—this might be fluid velocity if we are thinking about convection, or colour if we are thinking about animal markings.

In general the partial differential equation is defined on the domain  $\mathbb{R}^2 \times \Omega$ , where  $\Omega$  is a space representing some specific features of the model. For example, in a model for convection we take  $\Omega$  to be an interval which represents the depth of the fluid. In Section 4 we will study the visual cortex, where we take  $\Omega$  to be the circle  $S^1$ . However, to get an understanding of the problem we do not need to consider  $\Omega$  at this stage.

We assume that our plane has Euclidean symmetry, i.e. it is homogeneous and isotropic. This means that it is invariant under the Euclidean groups  $E(2)$  composed of all translations, rotations and reflections of the plane. Recall that this gives us an equivariance condition

$$\gamma f(u, \mu) = f(\gamma u, \mu) \quad \forall \gamma \in E(2) \quad (13)$$

and thus we have a trivial solution to the equation  $f(u, \mu) = 0$ , given by  $u = 0$ . We assume that the system undergoes a steady bifurcation at  $\mu = 0$ , where the trivial fixed point is stable for  $\mu < 0$  and unstable for  $\mu > 0$ .

Consider Fourier mode perturbations  $u(\mathbf{x}, t) = e^{\lambda t + i\mathbf{k} \cdot \mathbf{x}}$  to the zero pattern. Linearising the equations we obtain a dispersion relation, i.e. an expression for  $\lambda$  as a function of  $k = |\mathbf{k}|$ , and we want to consider the case where the zero solution first becomes unstable, i.e. when  $\lambda = 0$ . The dispersion curves often have a unique minimum at  $k = k_c$  where the pattern first becomes unstable. We want to consider the case when the bifurcation produces a regular lattice pattern, and to this end we assume that at the bifurcation point the  $u = 0$  solution is neutral to Fourier modes with a wave vector of this critical size,  $|\mathbf{k}| = k_c$ , and stable to all other modes.

At this point the problem is still fairly complicated, and we want to perform a centre manifold reduction to reduce it to something that we can analyse. However, to perform a centre manifold reduction we require that the decaying modes have growth rates bounded away from zero—this is clearly not the case here since a wave vector can be as close to the critical size as we like, so there are modes which decay infinitesimally slowly. We have a second problem, which is that even if we could perform the reduction, there are still infinitely many wave vectors of the critical size, and so our problem is still infinite dimensional.

We get around these problems by restricting our attention to a planar lattice. All wave vectors must then lie on the vertices of the lattice, and so we do away with both problems at once. The critical circle will only intersect a finite number of wave vectors, and any wave vector not on the critical circle will have a growth rate bounded away from zero.

There is no rigorous justification for this restriction to a lattice, but we can convince ourselves that it is reasonable. The lattice is a subgroup of the group of translations, and the set  $F$  of functions periodic on a lattice is the fixed-point subspace of that group of translations. Thus  $F$  is an invariant subspace of the partial differential equation (12), so solutions restricted to the lattice are solutions of the original system. We can now apply the centre manifold theorem, writing

$$u(\mathbf{x}, t) = \sum_{j=1}^n z_j(t) e^{i\mathbf{k}_j \cdot \mathbf{x}} + \text{c.c.}$$

where ‘c.c.’ represents the complex conjugate. The  $\mathbf{k}_j$  are the wave vectors lying on the critical circle, having magnitude  $k_c$ . Note that we only need to count half of the wave vectors on the critical circle, because the amplitude of the mode  $e^{-i\mathbf{k}_j \cdot \mathbf{x}}$  must be  $\bar{z}_j$  since  $u$  is real.

As  $\mu$  increases past zero the growth rate of the critical modes becomes positive, and we get

evolution equations for the  $z_j$  of the form

$$\dot{z} = g(z, \mu), \quad z \in \mathbb{C}^n \quad (14)$$

which we call *amplitude equations*. The zero solution is now  $z = 0$ , and the requirement that the bifurcation is steady becomes  $g(0, \mu) = 0$ . If we write  $z = \xi + i\eta$  then we can make the identification  $\mathbb{C}^n \equiv \mathbb{R}^{2n}$ , and we then also have  $Dg|_{(0, \mu)} = c(\mu)I$  with  $c(0) = 0$ .

The set of equations (14) inherit symmetry from the  $E(2)$  symmetry of the original problem—namely the finite group of reflections and rotations that preserve the lattice, called the *holohedry*  $H$  of the lattice, together with the translations. We can ‘factor out’ the lattice from the translation group, and the translations then form a torus group  $T^2 = S^1 \times S^1$ . The symmetry of the bifurcation problem is thus given by  $\Gamma = H \bowtie T^2$ , where ‘ $\bowtie$ ’ is the semi-direct product. For example, for a square lattice  $H = D_4$ , and for a hexagonal lattice  $H = D_6$ .

The set of equations also satisfy equivariance conditions

$$\gamma g(z, \mu) = g(\gamma z, \mu) \quad \forall \gamma \in \Gamma. \quad (15)$$

These allow us to write down the general form of the amplitude equations, in other words the normal form of the bifurcation.

### 3.2 Steady bifurcation on a square lattice

In this section we examine the solution branches that can appear in a steady bifurcation on a square lattice. Note that by choosing to analyse the situation in this way we have made two choices—the choice to restrict our attention to a lattice, and the choice of the lattice itself, in this case square over hexagonal. These may sound restrictive, but they are really quite reasonable. From observation we know that lattice patterns crop up often, and since we know that square patterns are seen in nature it seems sensible to choose a square lattice if we want to study them.

The symmetry group of a square lattice is  $D_4 \bowtie T^2$ . We rescale space so that our critical wavevectors have magnitude 1, and we choose to use the natural representation of  $D_4 \bowtie T^2$  so that there are two orthogonal wave vectors  $(1, 0)$  and  $(0, 1)$  and to leading order a solution looks like

$$u(\mathbf{x}, t) = z_1(t)e^{ix} + z_2(t)e^{iy} + \text{c.c.} \quad z_1, z_2 \in \mathbb{C}. \quad (16)$$

where  $\mathbf{x} = (x, y)$ . We want to consider the action of the fundamental representation of  $D_4 \bowtie T^2$  on  $\mathbb{C}^2$ . The group is generated by

- a rotation through  $\pi/2$ ,  $\rho$ , with action  $\rho : (x, y) \rightarrow (-y, x)$
- a reflection in  $x$ ,  $m$ , with action  $m : (x, y) \rightarrow (-x, y)$ , and
- translations  $\mathbf{p} \in T^2$ , whose action is given by  $\mathbf{p} : \mathbf{x} \rightarrow \mathbf{x} + \mathbf{p}$ .

We can deduce the actions of these generators on  $z_1, z_2$  by requiring that the general form of the equation (16) be unchanged under the symmetries.

The natural or *scalar* action of the Euclidean group on a function  $v(\mathbf{x})$  is given by

$$\gamma v(\mathbf{x}) = v(\gamma^{-1}\mathbf{x}), \quad \forall \gamma \in E(2), \forall \mathbf{x} \in \mathbb{R}^2.$$

The inverse is needed so that the action of the group on the space of functions is a homomorphism. We can verify this by considering the action of  $\sigma \in E(2)$  on  $w(\mathbf{x}) = v(\gamma^{-1}\mathbf{x})$ . There is another action called the *pseudoscalar* action, which acts as

$$\gamma v(\mathbf{x}) = \begin{cases} v(\gamma^{-1}\mathbf{x}) & \text{if } \gamma \text{ is a rotation or a reflection,} \\ -v(\gamma^{-1}\mathbf{x}) & \text{if } \gamma \text{ is a reflection.} \end{cases}$$

We will discuss this action later when we consider pseudoscalar patterns. For now we only consider scalar patterns.

In our example we have the symmetry group  $D_4 \rtimes T^2$ . A rotation acts on  $u$  as  $\rho u(\mathbf{x}, t) = u(\rho^{-1}\mathbf{x}, t)$ . In our representation we have

$$\rho^{-1} \begin{pmatrix} x \\ y \end{pmatrix} = \begin{pmatrix} 0 & 1 \\ -1 & 0 \end{pmatrix} \begin{pmatrix} x \\ y \end{pmatrix} = \begin{pmatrix} y \\ -x \end{pmatrix}, \quad (17)$$

and applying this to (16) gives

$$\rho u(\mathbf{x}, t) = z_1(t)e^{iy} + z_2(t)e^{-ix} + \bar{z}_1(t)e^{-iy} + \bar{z}_2(t)e^{ix}$$

We have not changed the general form of the solution, but the action of  $\rho$  has sent  $(z_1, z_2)$  to  $(\bar{z}_2, z_1)$ . Performing a similar analysis for  $m$  and  $p$  we find that

$$\begin{aligned} \rho : (z_1, z_2) &\rightarrow (\bar{z}_2, z_1) \\ m : (z_1, z_2) &\rightarrow (\bar{z}_1, z_2) \\ \mathbf{p} : (z_1, z_2) &\rightarrow (e^{-ip_1}z_1, e^{-ip_2}z_2). \end{aligned} \quad (18)$$

where  $\mathbf{p} = (p_1, p_2)$ . We can thus consider a real four-dimensional representation acting on  $\mathbb{C}^2 \equiv \mathbb{R}^4$ , where we write  $z_1 = \xi_1 + i\eta_1$  and  $z_2 = \xi_2 + i\eta_2$ , and consider the action on the four-dimensional amplitude vector  $(\xi_1, \eta_1, \xi_2, \eta_2)$ . We get the matrices

$$\begin{aligned} \theta(\rho) &= \begin{pmatrix} 0 & 0 & 1 & 0 \\ 0 & 0 & 0 & -1 \\ 1 & 0 & 0 & 0 \\ 0 & 1 & 0 & 0 \end{pmatrix}, & \theta(m) &= \begin{pmatrix} 1 & 0 & 0 & 0 \\ 0 & -1 & 0 & 0 \\ 0 & 0 & 1 & 0 \\ 0 & 0 & 0 & 1 \end{pmatrix}, \\ \theta(\mathbf{p}) &= \begin{pmatrix} \cos p_1 & \sin p_1 & 0 & 0 \\ -\sin p_1 & \cos p_1 & 0 & 0 \\ 0 & 0 & \cos p_2 & \sin p_2 \\ 0 & 0 & -\sin p_2 & \cos p_2 \end{pmatrix}. \end{aligned} \quad (19)$$

	Orbit representative	Isotropy subgroup	
Solution branch	$(z_1, z_2)$	and generators	$\dim \text{Fix}(\Sigma)$
Trivial solution	$(0, 0)$	$D_4 \rtimes T^2$	0
Rolls	$(\xi_1, 0)$	$D_2 \rtimes S^1$ $\{\rho^2, m, (p_1, 0)\}$	1
Squares	$(\xi_1, \xi_1)$	$D_4$ $\{\rho, m\}$	1
Bimodal	$(\xi_1, \xi_2), \xi_1 \neq \xi_2$	$D_2$ $\{\rho^2, m\}$	2

Table 2: Isotropy subgroups for a steady bifurcation on a square lattice using the fundamental representation.

It is then simple to check that the only matrices that commute with all the generators are multiples of the identity, so that representation acts absolutely irreducibly and we can apply the equivariant branching lemma. To do this we need to find the isotropy subgroups and see which ones are one-dimensional. This information is summarised in Table 2. We notice that the solution branches with one-dimensional fixed-point subspaces are rolls and squares, and the equivariant branching lemma guarantees that they will occur in bifurcations.

We can now use the the equivariance conditions given by (15) to deduce the general form of the amplitude equations for  $z_1(t)$  and  $z_2(t)$ . To linear order we can expand the equations as

$$\begin{aligned}\dot{z}_1 &= \mu_1 z_1 + a_1 \bar{z}_1 + b_1 z_2 + c_1 \bar{z}_2 \\ \dot{z}_2 &= \mu_2 z_2 + a_2 \bar{z}_2 + b_2 z_1 + c_2 \bar{z}_1\end{aligned}\tag{20}$$

where  $\mu_1, \mu_2$  are real bifurcation parameters and  $a_j, b_j$  and  $c_j$  are constants. In fact it is clear that these must all be zero, or we would not have a steady bifurcation at the origin. However, we will pretend for a while that we don't know this, so that we can see the effect of the equivariance conditions on the form of the equations.

First consider translation, and recall that the effect of a translation is  $\mathbf{p} : (z_1, z_2) \rightarrow (e^{-ip_1} z_1, e^{-ip_2} z_2)$ . For the equations to be equivariant we must have

$$\begin{aligned}e^{-ip_1}(\mu_1 z_1 + a_1 \bar{z}_1 + b_1 z_2 + c_1 \bar{z}_2) &= \mu_1 e^{-ip_1} z_1 + a_1 e^{ip_1} \bar{z}_1 + b_1 e^{-ip_2} z_2 + c_1 e^{ip_2} \bar{z}_2 \\ e^{-ip_2}(\mu_2 z_2 + a_2 \bar{z}_2 + b_2 z_1 + c_2 \bar{z}_1) &= \mu_2 e^{-ip_2} z_2 + a_2 e^{ip_2} \bar{z}_2 + b_2 e^{-ip_1} z_1 + c_2 e^{ip_1} \bar{z}_1\end{aligned}$$

and so the coefficients  $a_j, b_j$  and  $c_j$  must all be zero as expected. We can then apply rotation equivariance, the effect of which is  $\rho : (z_1, z_2) \rightarrow (\bar{z}_2, z_1)$ , and we get

$$\mu_2 \bar{z}_2 = \mu_1 \bar{z}_2$$

$$\mu_1 z_1 = \mu_2 z_1, \quad (21)$$

so we must have  $\mu_1 = \mu_2$ . We could expand the amplitude equations to higher order, say to cubic order, and repeat the process to find the normal form of the bifurcation. However, this would get very messy very quickly. It is easier to consider each term at higher order separately to see which ones can have non-zero coefficients, and only then apply the equivariance conditions to determine the restrictions on the coefficients.

At quadratic order we find that all coefficients must be zero to satisfy translation equivariance. For example, consider the term  $|z_1|^2$ . For the equations to be equivariant we would need

$$e^{-ip_1} |z_1|^2 = |e^{-ip_1} z_1|^2 \quad \forall p_1 \in \mathbb{R}$$

but this is clearly not the case, so there can be no  $|z_1|^2$  term. We can similarly deduce that there can be no other quadratic terms in the equations.

At cubic order we can again apply translation equivariance to deduce that many of the coefficients must be zero. Taking this into account, we find that to cubic order the amplitude equations must take the form

$$\begin{aligned} \dot{z}_1 &= \mu z_1 - a_1 |z_1|^2 z_1 - b_1 |z_2|^2 z_1 \\ \dot{z}_2 &= \mu z_2 - a_2 |z_2|^2 z_2 - b_2 |z_1|^2 z_2 \end{aligned}$$

with  $a_1, a_2, b_1, b_2 \in \mathbb{C}$ . Applying reflection equivariance,  $m : (z_1, z_2) \rightarrow (\bar{z}_1, z_2)$ , to the first equation gives

$$\mu \bar{z}_1 - \bar{a}_1 |z_1|^2 \bar{z}_1 - \bar{b}_1 |z_2|^2 \bar{z}_1 = \mu \bar{z}_1 - a_1 |z_1|^2 \bar{z}_1 - b_1 |z_2|^2 \bar{z}_1,$$

so we must have  $a_1, b_1 \in \mathbb{R}$ . Applying rotation equivariance to the second equation gives

$$\mu z_1 - a_1 |z_1|^2 z_1 - b_1 |z_2|^2 z_1 = \mu z_1 - a_2 |z_1|^2 z_1 - b_2 |z_2|^2 z_1$$

and so we must have  $a_1 = a_2 = a$  and  $b_1 = b_2 = b$ . We can then write the amplitude equations as

$$\begin{aligned} \dot{z}_1 &= \mu z_1 - a |z_1|^2 z_1 - b |z_2|^2 z_1 \\ \dot{z}_2 &= \mu z_2 - a |z_2|^2 z_2 - b |z_1|^2 z_2. \end{aligned}$$

These equations have a property which turns out to be very convenient. We can shift our origins to choose  $z_1$  and  $z_2$  to be real initially, and then because all of the coefficients in the amplitude equations are real, they will be real for all  $t$ . If we rewrite the amplitude equations taking  $z_1, z_2 \in \mathbb{R}$  we get

$$\begin{aligned} \dot{z}_1 &= \mu z_1 - a z_1^3 - b z_2^2 z_1 \\ \dot{z}_2 &= \mu z_2 - a z_2^3 - b z_1^2 z_2. \end{aligned} \quad (22)$$

These have exactly the same form as for the bifurcation in a square box, equations (9), and thus we can use the same analysis for finding the fixed points and finding their stabilities.

We expect to find a trivial fixed point at the origin, corresponding to a uniform zero solution. We then have solutions of the form  $(z, 0)$  and  $(0, z)$  with  $z^2 = \mu/a$  which correspond to uniform rolls, and solutions of the form  $(z, \pm z)$  with  $z^2 = \mu/(a+b)$  which correspond to squares. Notice that we don't see the bimodal solution that we would expect from our consideration of the isotropy subgroups in Table 2. This is an artifact of truncating our equations at cubic order—had we gone to quintic order we would also have solutions of this type.

The stability of the various pattern modes can be seen by considering Figure 1, where the label  $R$  now corresponds to rolls and  $S$  corresponds to squares. We see that the most interesting areas of the  $(a, b)$  plane are in  $a > 0$  and  $b < -a$ . Here the system bifurcates as we increase  $\mu$  above zero, and a steady pattern of either rolls or squares emerges.

### 3.3 Steady bifurcation on a hexagonal lattice

A hexagonal lattice allows much more scope for pattern formation. The dual lattice is generated by three vectors  $\mathbf{k}_1, \mathbf{k}_2, \mathbf{k}_3$  which satisfy  $\mathbf{k}_1 + \mathbf{k}_2 + \mathbf{k}_3 = 0$ , as in Figure 3. Because the wave vectors are linearly dependant we have the possibility for resonance. A first approximation for our solution is

$$u(\mathbf{x}, t) = \sum_{j=1}^3 z_j(t) e^{i\mathbf{k}_j \cdot \mathbf{x}} + \text{c.c.} \quad (23)$$

where  $z_1, z_2$  and  $z_3$  are the amplitudes of the three plane waves. The symmetry group of the lattice is  $D_6 \rtimes T^2$ , which is generated by

- a rotation by  $\pi/3$ ,  $\rho$ ,
- a reflection in the vertical axis,  $m$ , and
- translations  $\mathbf{p} \in T^2$ .

The actions of the generators on the center manifold  $\mathbb{C}^3$  are as follows:

$$\begin{aligned} \rho : (z_1, z_2, z_3) &\rightarrow (\bar{z}_2, \bar{z}_3, \bar{z}_1) \\ m : (z_1, z_2, z_3) &\rightarrow (z_1, z_3, z_2) \\ \mathbf{p} : (z_1, z_2, z_3) &\rightarrow (e^{-i\mathbf{k}_1 \cdot \mathbf{p}} z_1, e^{-i\mathbf{k}_2 \cdot \mathbf{p}} z_2, e^{-i\mathbf{k}_3 \cdot \mathbf{p}} z_3) \end{aligned} \quad (24)$$

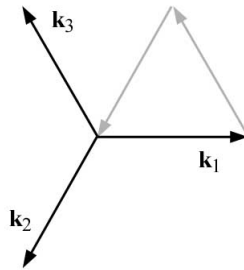


Figure 3: Generating wave vectors for the hexagonal lattice.

	Orbit representative	Isotropy subgroup $\Sigma$	
Solution branch	$(z_1, z_2, z_3)$	and generators	$\dim \text{Fix}(\Sigma)$
Trivial solution	$(0, 0, 0)$	$D_6 \rtimes T^2$	0
Rolls	$(\xi_1, 0, 0)$	$D_2 \rtimes S^1$ $\{\rho^3, m, (0, p_2)\}$	1
Up-hexagons	$(\xi_1, \xi_1, \xi_1), \xi_1 > 0$	$D_6$ $\{\rho, m\}$	1
Down-hexagons	$(\xi_1, \xi_1, \xi_1), \xi_1 < 0$	$D_6$ $\{\rho, m\}$	1
Rectangles	$(\xi_1, \xi_2, \xi_2)$	$D_2$ $\{\rho^3, m\}$	2
Triangles	$(z_1, z_1, z_1)$	$D_3$ $\{\rho^2, m\}$	2

Table 3: Isotropy subgroups for a steady bifurcation on a hexagonal lattice using the fundamental representation

Proceeding as we did for the square lattice, we can consider the representation over  $\mathbb{R}^6$  by writing  $z_j = \xi_j + \eta_j$ . Again we find that the representation is absolutely irreducible, and so we can use the equivariant branching lemma to make predictions about the steady bifurcations at the origin. The isotropy subgroups of  $D_6 \rtimes T^2$  are given in Table 3, and we notice that there are two isotropy subgroups with one-dimensional fixed-point subspaces, which correspond to rolls and to hexagons. Thus we expect to see two solution branches at the bifurcation point, one of rolls and one of hexagons.

We can now use equivariance conditions to deduce the form of the amplitude equations. We should note that the combination  $\bar{z}_2 \bar{z}_3$  transforms under translations  $\mathbf{p}$  to  $\bar{z}_2 \bar{z}_3 e^{i(\mathbf{k}_2 + \mathbf{k}_3) \cdot \mathbf{x}} = \bar{z}_2 \bar{z}_3 e^{-i\mathbf{k}_1 \cdot \mathbf{x}}$ , i.e. it transforms in the same way as  $z_1$ . This means that  $\bar{z}_2 \bar{z}_3$  can appear in the amplitude equation for  $z_1$ . We should also note that we can't use the trick of shifting the origin to make all the amplitudes real, because moving the origin so that  $z_1$  and  $z_2$  are real will still leave  $z_3$  complex in general.

Other than that, the calculation proceeds much as it did for bifurcations on a square lattice. Up to cubic order, we find that the amplitude equations are

$$\begin{aligned}
\dot{z}_1 &= \mu z_1 + a \bar{z}_2 \bar{z}_3 - b |z_1|^2 z_1 - c(|z_2|^2 + |z_3|^2) z_1 \\
\dot{z}_2 &= \mu z_2 + a \bar{z}_3 \bar{z}_1 - b |z_2|^2 z_2 - c(|z_3|^2 + |z_1|^2) z_2 \\
\dot{z}_3 &= \mu z_3 + a \bar{z}_1 \bar{z}_2 - b |z_3|^2 z_3 - c(|z_1|^2 + |z_2|^2) z_3.
\end{aligned} \tag{25}$$

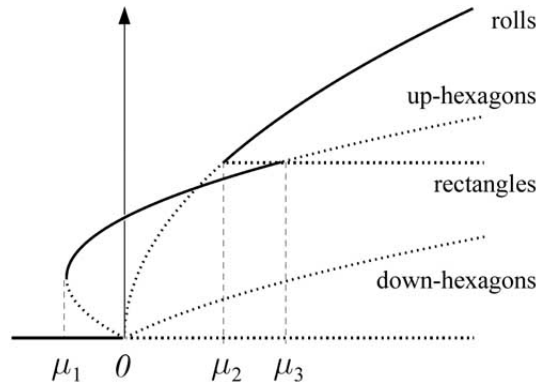


Figure 4: Typical bifurcation diagram for the steady bifurcation on a hexagonal lattice in the fundamental representation, in the case  $a > 0$  and  $b < c$ . Branches where all three components  $z_1, z_2, z_3$  are stable are indicated by solid lines, and branches with at least one component unstable by dashed lines. The vertical axis represents  $|z_1|$ , and we have projected the branches for all solutions onto this line.

With these equations we can find the fixed points and then use perturbation methods to determine the stability of the various solutions. As before, we do not find all possible solutions using this method—we don't see a solution corresponding to triangles, for example. The stability analysis is quite messy and so we'll skip it, but a typical bifurcation diagram is shown in Figure 4. Note that the bifurcation diagram predicts hysteresis in the system, when there is more than one stable pattern for a given value of  $\mu$ . Increasing  $\mu$  slowly past the point marked  $\mu_3$  will prompt a change from a hexagonal pattern to a rolls pattern, but if we then decrease  $\mu$  slowly again we do not see the hexagons reappear until  $\mu$  is below the point marked  $\mu_2$ . This kind of behaviour was observed experimentally by Dubois, Bergé and Wesfried in 1978 in a convection experiment.

In summary, then, we have seen that we can classify the patterns that emerge from a bifurcation in two ways. First we can look at the isotropy subgroups, and use the equivariant branching lemma to deduce which patterns are guaranteed to emerge at a bifurcation. This has the advantage that we will be able to classify every possible pattern, but it does not give us any information about stability—we do not know which pattern will be selected. Alternatively we can use equivariance to deduce the normal form of the amplitude equations, and then go on to classify the solutions and their stabilities. This gives us much more information about each solution, but we can easily miss possible solutions if we do not go to a high enough order.

### 3.4 Pseudoscalar patterns

We noted earlier that as well as the natural scalar action on a function, the Euclidean group  $E(2)$  also has a pseudoscalar action given by

$$\gamma v(\mathbf{x}) = \begin{cases} v(\gamma^{-1}\mathbf{x}) & \text{if } \gamma \text{ is a rotation or a reflection,} \\ -v(\gamma^{-1}\mathbf{x}) & \text{if } \gamma \text{ is a reflection.} \end{cases}$$

Most physical systems that are invariant under the Euclidean group are governed by a partial differential equation that is invariant under the scalar action of the group, but some are governed by an equation which is invariant under the pseudoscalar action. A well-known example are the two-dimensional Navier-Stokes equations for fluid flow in the plane. The pseudoscalar action gives rise to new patterns.

Consider the case of the bifurcation on the hexagonal lattice, where we write a first approximation to the solutions as

$$u(\mathbf{x}, t) = \sum_{j=1}^3 z_j(t) e^{i\mathbf{k}_j \cdot \mathbf{x}} + \text{c.c.}$$

As before the symmetry group of the problem is  $D_6 \rtimes T^2$ , but the actions of the generators are different. The translations act in the same way, but now a reflection acts as

$$m : (z_1, z_2, z_3) \rightarrow (-z_1, -z_3, -z_2).$$

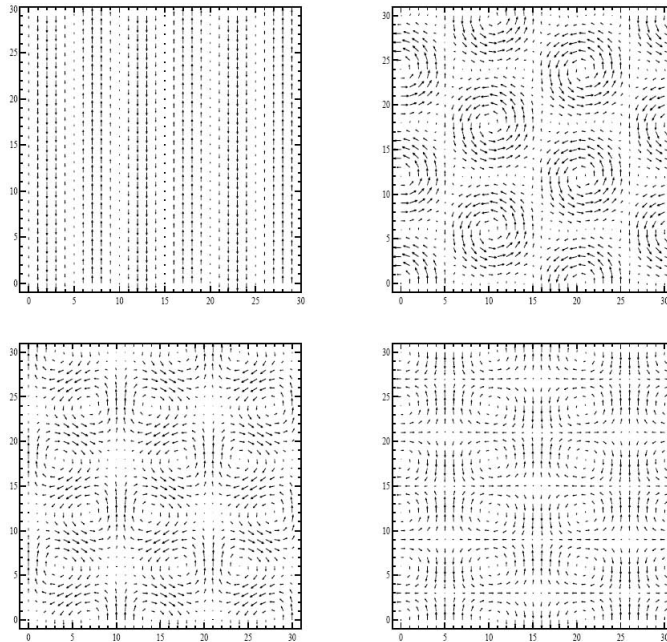


Figure 5: Pseudoscalar patterns with axial branches for bifurcation on a hexagonal lattice, plotted as velocity fields. Top left anti-rolls, top right anti-hexagons, bottom left anti-triangles and bottom-right anti-rectangles.

The additional minus sign has the effect of prohibiting quadratic terms in the amplitude equations. To cubic order they now look like

$$\begin{aligned} \dot{z}_1 &= \mu z_1 - b|z_1|^2 z_1 - c(|z_2|^2 + |z_3|^2) z_1 \\ \dot{z}_2 &= \mu z_2 - b|z_2|^2 z_2 - c(|z_3|^2 + |z_1|^2) z_2 \\ \dot{z}_3 &= \mu z_3 - b|z_3|^2 z_3 - c(|z_1|^2 + |z_2|^2) z_3. \end{aligned} \quad (26)$$

The most important differences with the scalar case are in the predicted patterns. Consider the solution

$$u_{AR}(x, y) = a(e^{ix} + e^{-ix}), \quad (27)$$

with  $a \in \mathbb{R}$  constant. In the scalar case this was a roll solution with isotropy subgroup  $D_2 \rtimes S^1$ , but in the pseudoscalar case a reflection takes  $u_{AR}$  to  $-u_{AR}$ , so a reflection is no longer a symmetry of the solution! However, the combination of a reflection with a translation  $x \rightarrow x + \pi$  is a symmetry, and this leads to what is called a *twisted* symmetry group, denoted  $D_2^- \rtimes S^1$ . The new pattern is called anti-rolls.

The expression for the solution in (27) is no different to the scalar case, but the different symmetry group leads to a different interpretation in physical space. Orientation becomes important, so instead of plotting the pattern as contours we instead treat the solution as a streamfunction and plot planar velocity vectors  $\mathbf{v} = (v_1, v_2)$ , given by  $(v_1, v_2) = (\partial u / \partial y, -\partial u / \partial x)$ . An anti-rolls pattern is shown in Figure 5.

Similarly the hexagon patterns are replaced with an oriented pattern called anti-hexagons, with symmetry group  $\mathbb{Z}^6$  comprised solely of rotations. What is even more surprising, though, is that with the new symmetry groups we get two more isotropy subgroups with one-dimensional fixed-point subspaces. These are  $D_3$  and  $D_2$ , which correspond to anti-triangles and anti-rectangles respectively. Examples of all of these patterns are shown in Figure 5.

## 4 Hallucination Patterns in the Visual Cortex

In *The Doors of Perception*, in which Aldous Huxley describes his experiences following the ingestion of four tenths of a gram of mescaline, the author writes

“Half an hour after swallowing the drug I became aware of a slow dance of golden lights. A little later there were sumptuous red surfaces swelling and expanding from bright nodes of energy that vibrated with a continuously changing, patterned life. At another time the closing of my eyes revealed a complex of grey structures, within which pale blueish spheres kept emerging into intense solidity and, having emerged, would slide noiselessly upwards, out of sight.”

Visions of regular geometric patterns are a common theme among reports of people who have taken hallucinogenic drugs. In 1966 Klüver studied the effects of mescaline on the human visual system,

and classified the most commonly reported patterns into four groups: (a) tunnels and funnels, (b) spirals, (c) lattices, including honeycombs and checkerboards, and (d) cobwebs. These patterns can be generated in other ways, the most readily accessible of which is to close your eyes and apply firm pressure to the eyeballs with your fingers for about ten seconds.

Most reports agree that the phenomenon do not move with the eyes. This suggests that they are not generated in the eyes, but in the brain—specifically, in the visual cortex. The visual cortex in humans is fairly large, occupying a significant portion of the frontal lobe of the brain. It is made of of five parts with distinct functions, denoted V1, . . . , V5. An interesting conjecture is that hallucinatory patterns are generated in the primary visual cortex, V1. The function of V1 is contour and edge detection—the receptors are sensitive not only to the presence or absence of light, but also to orientation.

Recent advances in brain imaging using electrodes and chemical dyes have yielded important information about the structure of V1. It is suspected that V1 in humans is roughly square, with sides of approximately 40mm. The mapping from the retina to V1 is smooth, in the sense that nearby cells in the retina stimulate nearby cells in V1. V1 is divided into patches called hypercolumns roughly 1-2mm in size, and each hypercolumn contains cells capable of detecting contours of any orientation.

#### 4.1 The human retino-cortical map

An important first step is to calculate what hallucinations look like in the coordinates of V1, rather than in retinal, or equivalently visual field, coordinates. We use polar coordinates  $(r, \theta)$  to denote visual field coordinates and Cartesian  $(x, y)$  coordinates to denote positions in V1. Cells in V1 have a roughly uniform packing density  $\rho$ , so that the number of cells in an area  $dxdy$  is  $\rho dxdy$ . The packing density of retinal cells is denoted  $\rho_R$  so that the number of cells in a retinal area  $rdrd\theta$  is  $\rho_R r dr d\theta$ . It is known that there are far more cells in areas corresponding to the centre of the visual field than there are at the edges—roughly,  $\rho_R$  satisfies an inverse square rule:

$$\rho_R = \frac{1}{(1 + \epsilon r)^2}$$

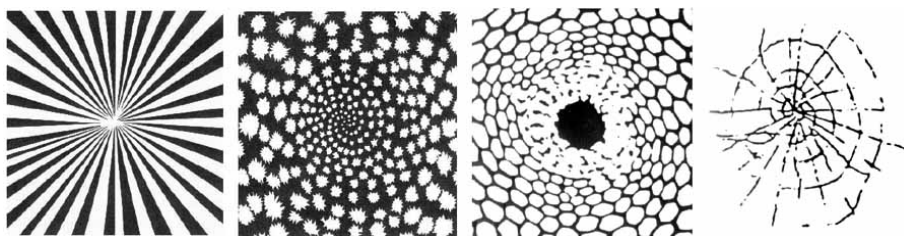


Figure 6: Commonly reported hallucination patterns. A funnel and a spiral pattern generated by LSD, and a honeycomb and cobweb generated by marijuana.

where  $\epsilon$  is a constant. From this we can determine the Jacobian of the transformation from visual field to V1 coordinates, and hence obtain  $(x, y)$  as a function of  $(r, \theta)$ . The resulting coordinate transformation is:

$$x = \frac{\alpha}{\epsilon} \log(1 + \epsilon r), \quad y = \frac{\beta r \theta}{1 + \epsilon r} \quad (28)$$

where  $\alpha, \beta$  are constants. There is an important limiting case, namely the case when we are far from the fovea. This corresponds to  $\epsilon r \gg 1$ . Sufficiently far from the fovea the transformation becomes

$$x = \frac{\alpha}{\epsilon} \log \epsilon r, \quad y = \frac{\beta \theta}{\epsilon}. \quad (29)$$

It turns out that this is a good approximation for all of the retina except the cells near the very centre, and thus using this form of the transformation we can calculate the effect that the transformation has on circles, rays and logarithmic spirals. Circles are given in visual fields coordinates by  $r = \text{constant}$ , which corresponds to  $x = \text{constant}$ . Thus circles are vertical lines in V1. Rays are given by  $\theta = \text{constant}$ , which corresponds to  $y = \text{constant}$ . So rays correspond to horizontal lines in V1. Finally, logarithmic spirals are given in visual field coordinates by  $r = \exp \theta$ , which corresponds in V1 coordinates to  $x, y \propto \theta$ . Thus logarithmic spirals correspond to oblique lines in V1.

This should make us feel optimistic! We know that stripes are a very commonly occurring pattern, and the analysis that we've just performed tells us that stripes of neural activity in V1 can generate spirals, circles and rays in the visual field, all of which are key components of Klüver's hallucinatory form constants. However, we need to investigate further to see how the more intricate patterns, such as cobwebs, can arise.

## 4.2 Modelling V1

The function of a single hypercolumn is to determine whether a contour occurs at a specific point in the retinal image, and what its orientation is. To accomplish this, each cell in a hypercolumn responds to a different orientation, and all pairs of cells are connected by an inhibitory coupling so that when a contour is detected with a certain orientation it suppresses the cells looking for different orientations.

The connections between hypercolumns are more interesting, because cells in different hypercolumns are only connected if they share the same orientation, and moreover the axons supporting those connections are orientated in the same direction as the orientation preference for the cells that they connect. This is illustrated schematically in Figure 7. The lateral connections are much weaker than the local connections.

It is this intricate coupling which gives rise to the interesting patterns which can arise. We model V1 as a continuum limit, and take our phase space to be  $\mathbb{R}^2 \times S^1$  where a vector  $\mathbf{x} = (x, y) \in \mathbb{R}^2$  represents the position of a hypercolumn, and the angle  $\phi \in S^1$  represents orientations in that hypercolumn, with the directions  $\phi$  and  $\phi + \pi$  identified. In this model we can summarise the connections between cells as:

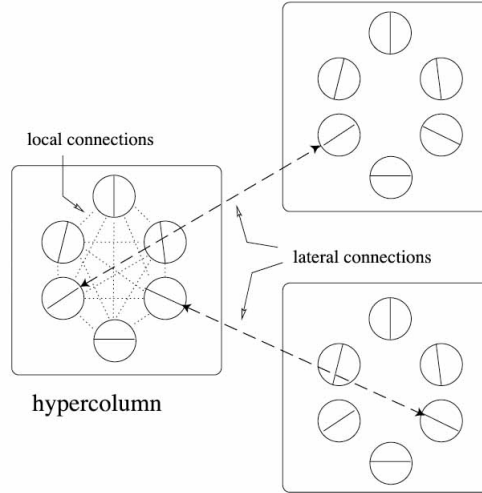


Figure 7: Schematic diagram of connections in the primary visual cortex. Faint dotted lines represent local, inhibitory connections whereas dashed lines represent lateral, excitatory connections.

- Local, inhibitory connections connect cells at the *same*  $\mathbf{x}$  and *different*  $\phi$ .
- Lateral, excitatory connections connect cells at *different*  $\mathbf{x}$  and the *same*  $\phi$ , in a direction parallel to  $\phi$ .

We model the level of neural activity by an activity variable  $a(\mathbf{r}, \phi, t)$ , satisfying a governing partial differential equation. Early work by Ermentrout and Cowan predicted *some* of Klüver's form constants, but not all of them. Their work did not take the orientation preference of cortical cells into account. Here we use a generalisation of the Wilson-Cowan equation,

$$\frac{\partial a(\mathbf{r}, \phi, t)}{\partial t} = -\alpha a(\mathbf{r}, \phi, t) + \frac{\mu}{\pi} \int_0^\pi \int_{\mathbb{R}^2} w(\mathbf{r}, \phi, \mathbf{r}', \phi') \sigma[a(\mathbf{r}', \phi', t)] d\mathbf{r}' d\phi' + h(\mathbf{r}, \phi, t), \quad (30)$$

where  $\alpha$  and  $\mu$  are decay and coupling coefficients,  $w(\mathbf{r}, \phi, \mathbf{r}', \phi')$  is a function representing the strength of the connection between cells at  $(\mathbf{r}, \phi)$  and  $(\mathbf{r}', \phi')$ ,  $h(\mathbf{r}, \phi, t)$  is an external forcing and  $\sigma[z]$  is the smooth function

$$\sigma[z] = \frac{1}{1 + e^{-kz}} \quad (31)$$

for  $k$  a constant. In fact we can scale  $\sigma$  and add a constant to it without affecting the equations, so we choose a constant to ensure that  $\sigma[0] = 0$ . This ensures that the zero state  $a = 0$  is a solution of the unforced equations.

If we use the notation  $s = |\mathbf{r} - \mathbf{r}'|$  then we can decompose the function  $w(\mathbf{r}, \phi, \mathbf{r}', \phi')$  as a sum of local and lateral interactions, which we write as

$$w(\mathbf{r}, \phi, \mathbf{r}', \phi') = w_{loc}(\phi - \phi') \delta(\mathbf{r} - \mathbf{r}') + \beta w_{lat}(\mathbf{r} - \mathbf{r}', \phi) \delta(\phi - \phi') \quad (32)$$

with

$$w_{lat}(\mathbf{r} - \mathbf{r}', \phi) = \hat{w}_{lat}(\mathbf{r} - \mathbf{r}') \delta(\mathbf{r} - \mathbf{r}' - s \mathbf{e}_\phi).$$

Here  $\delta(-)$  is the Dirac delta function,  $\mathbf{e}_\phi$  is a unit vector in the  $\phi$  direction and  $\beta$  is a coupling parameter representing the strength of the lateral connections as compared to the local connections. Typically we take  $\beta$  to be small. Note that although the local connections are homogeneous and isotropic, the lateral connections depend on  $\phi$ , so they are not isotropic.

### Euclidean symmetry

The  $\phi$ -dependence of the lateral connections introduces an anisotropy into the system. The network of connections is not invariant under the standard action of  $E(2)$ , but is invariant under an altered representation. The full symmetry group is generated by

- rotations  $\theta$ , acting as  $\theta : (\mathbf{x}, \phi) \rightarrow (R_\theta \mathbf{x}, \phi + \theta)$ ,
- a reflection  $m$ , acting as  $m : (x, y, \phi) \rightarrow (x, -y, -\phi)$ , and
- translations  $\mathbf{p}$ , acting as  $\mathbf{p} : (\mathbf{x}, \phi) \rightarrow (\mathbf{x} + \mathbf{p}, \phi)$ .

The form of the rotation follows from the anisotropy of the lateral connections. If we just rotated V1 then the lateral connections would connect cells of the wrong orientation, and so we compensate by also translating the orientation  $\phi$  to  $\phi + \theta$ . This is known as a *twist-shift* representation. It is easy enough to check that (32) is unchanged under this action of the Euclidean group. This invariance translates into *equivariance* of the governing equation.

### 4.3 Linearization

Substituting (32) into the modified Wilson-Cowan equation (30) we find that, for no external forcing,

$$\begin{aligned} \frac{\partial a(\mathbf{r}, \phi, t)}{\partial t} = & -\alpha a(\mathbf{r}, \phi, t) + \mu \left[ \frac{1}{\pi} \int_0^\pi w_{loc}(\phi - \phi') \sigma[a(\mathbf{r}, \phi', t)] d\phi' \right. \\ & \left. + \beta \int_{\mathbb{R}^2} w_{lat}(\mathbf{r} - \mathbf{r}', \phi) \sigma[a(\mathbf{r}', \phi, t)] d\mathbf{r}' \right] \end{aligned} \quad (33)$$

Before analysing the model described by equation (33) it is useful to consider a limiting case, namely the ring model of orientation tuning.

#### The ring model of orientation tuning

This model neglects all lateral connections, by setting  $\beta = 0$  in (33). This gives us a simpler equation,

$$\frac{\partial a(\mathbf{r}, \phi, t)}{\partial t} = -\alpha a(\mathbf{r}, \phi, t) + \frac{\mu}{\pi} \int_0^\pi w_{loc}(\phi - \phi') \sigma[a(\mathbf{r}, \phi', t)] d\phi'. \quad (34)$$

We can then linearize about  $a \equiv 0$  and consider perturbations of the form  $a(\mathbf{r}, \phi, t) = e^{\lambda t} a(\mathbf{r}, \phi)$ . This gives us an eigenvalue equation

$$\lambda a(\mathbf{r}, \phi) = -\alpha a(\mathbf{r}, \phi) + \frac{\mu}{\pi} \int_0^\pi w_{loc}(\phi - \phi') \sigma_1 a(\mathbf{r}, \phi') d\phi' \quad (35)$$

where  $\sigma_q = d\sigma[z]/dz$ , evaluated at  $z = 0$ . Finally we can postulate Fourier series expansions for  $a$  and  $w_{loc}$  of the form  $a = \sum z_m(\mathbf{r})e^{2im\phi} + c.c.$  and  $w_{loc}(\phi) = \sum W_n e^{2in\phi}$ . These give us a dispersion relation for  $\lambda$ ,

$$\lambda = -\alpha + \mu\sigma_1 W_m, \quad (36)$$

where we have used the orthogonality of the set  $e^{in\phi}$  under integration over a period  $\pi$ . If we let  $W_p$  be the coefficient of the strongest Fourier mode in  $w_{loc}$  then it is obvious from our dispersion relation that the zero state  $a(\mathbf{r}, \phi) \equiv 0$  is stable to perturbations for sufficiently small  $\mu$ , but becomes unstable to modes of the form  $a(\mathbf{r}, \phi) = z(\mathbf{r})e^{2ip\phi} + \bar{z}(\mathbf{r})e^{-2ip\phi}$  when  $\mu$  increases past the critical value  $\mu_c = \alpha/\sigma_1 W_p$ .

We run into a potentially thorny issue here. Recall that  $\mu$  was defined as a coupling constant in the modified Wilson-Cowan equation (30). What do we mean when we talk about  $\mu$  increasing—surely it is a built-in part of the equations, and so cannot change? This is true, but we are rescued by the presence of  $\sigma_1$ . If  $\sigma_1$  were to increase, this would decrease the critical value  $\mu_c$  at which the bifurcation occurs—perhaps even bringing it lower than  $\mu$ . So what does it mean for  $\sigma_1$  to increase? Recall that  $\sigma_1$  is the derivative of the function  $\sigma[z]$  at zero, which loosely represents the ‘excitability’ of the visual cortex for different levels of neural activity. If we were to have a constant non-zero forcing  $h(\mathbf{r}, \phi, t) = h_0$  in equation (30) then the homogeneous state would be non-zero,  $a(\mathbf{r}, \phi, t) = a_0$ , with  $\sigma_1 = \sigma'(a_0)$ . Thus varying the forcing  $h_0$  corresponds to varying  $\sigma_1$ , and making the visual cortex more ‘excitable’. Indeed, it is conjectured that this is one of the effects of hallucinogenic drugs!

Now if we write  $z(\mathbf{r})$  in polar coordinates,  $z(\mathbf{r}) = Z(\mathbf{r})e^{-2i\phi(\mathbf{r})}$ , then we find that  $a(\mathbf{r}, \phi) = Z(\mathbf{r})\cos[2(p\phi - \phi(\mathbf{r}))]$ . Thus at each point  $\mathbf{r}$ , the maximum response occurs at the orientation  $\phi = \phi(\mathbf{r}) + k\pi/p$ , with  $k = 0, 1, \dots, p-1$  for  $p \neq 0$ .

The most interesting cases from a biological perspective are  $p = 0$  and  $p = 1$ . In the first case there is no orientation preference at all. In the second case the instability is unimodal with respect to  $\phi$ , i.e. there is a peak at a certain value of  $\phi$ . We can interpret this biologically to infer the existence of a contour with a definite orientation at that point. This will be important later.

### Linearization of the Wilson-Cowan equation

We now linearize equation (33) about the zero state, and introduce small perturbations  $a(\mathbf{r}, \phi, t) = e^{\lambda t} a(\mathbf{r}, \phi)$ . This gives us the eigenvalue equation

$$\lambda a(\mathbf{r}, \phi) = -\alpha a(\mathbf{r}, \phi) + \sigma_1 \mu \left[ \frac{1}{\pi} \int_0^\pi w_{loc}(\phi - \phi') a(\mathbf{r}, \phi') d\phi' + \beta \int_{\mathbb{R}^2} w_{lat}(\mathbf{r} - \mathbf{r}', \phi) a(\mathbf{r}', \phi) d\mathbf{r}' \right]. \quad (37)$$

By translation symmetry we can write the activity variable as

$$a(\mathbf{r}, \phi) = u(\phi - \varphi) e^{i\mathbf{k}\cdot\mathbf{r}} + c.c. \quad (38)$$

where  $\mathbf{k} = q(\cos \varphi, \sin \varphi)$ , and we find that  $u$  satisfies

$$\lambda u(\phi) = -\alpha u(\phi) + \sigma_1 \mu \left[ \frac{1}{\pi} \int_0^\pi w_{loc}(\phi - \phi') u(\phi') d\phi' + \beta \tilde{w}_{lat}(\mathbf{k}, \phi + \varphi) u(\phi) \right], \quad (39)$$

where  $\tilde{w}_{lat}(\mathbf{k}, \phi)$  is the Fourier transform of  $w_{lat}(\mathbf{r}, \phi)$ . Since we know that the function  $w$  is Euclidean invariant, the symmetries of the system then restrict the solutions of the eigenvalue equation (39).

This happens in two ways:

- (i) Due to rotation invariance,  $\lambda$  and  $u(\phi)$  can only depend on the magnitude  $q = |\mathbf{k}|$  of the wave vector  $\mathbf{k}$ . Thus we have an infinite degeneracy.
- (ii) Due to reflection invariance, the space of eigenfunctions of the form

$$V_{\mathbf{k}} = \{u(\phi - \varphi)e^{i\mathbf{k}\cdot\mathbf{r}} + c.c. : u(\phi + \pi) = u(\phi) \text{ and } u \in \mathbb{C}\} \quad (40)$$

decomposes into two invariant subspaces  $V_{\mathbf{k}}^+$  and  $V_{\mathbf{k}}^-$  which correspond to even and odd  $u(\phi)$  respectively.

To see this let  $m_{\mathbf{k}}$  denote reflection about the wave vector  $\mathbf{k}$ , so that  $m_{\mathbf{k}}\mathbf{k} = \mathbf{k}$ . Then  $m_{\mathbf{k}}a(\mathbf{r}, \phi) = a(m_{\mathbf{k}}\mathbf{r}, 2\phi - \phi) = u(\varphi - \phi)e^{i\mathbf{k}\cdot\mathbf{r}} + c.c..$  Since  $m_{\mathbf{k}}$  is a reflection, any space on which it acts decomposes into two subspaces—one on which it acts as  $I$  and one on which it acts as  $-I$ .

From here we can proceed to analyse the eigenvalue equation (39) to find the possible eigenvalues and their stabilities. To do this we use degenerate perturbation theory, taking the ring model of orientation tuning as our base state. We work in the  $p = 1$  case, so that the sensitivity to orientation is unimodal. The actual analysis is long and tedious so we will skip it, and instead just summarise the main conclusions:

- When the zero state loses stability at  $\mu = \mu_c$ , it becomes unstable to modes whose wave vector  $\mathbf{k}$  has magnitude  $q_c$ . As noted in (i) above there are infinitely many such modes. Later we will reduce this to a finite number of modes by demanding that solutions be double periodic on a lattice.
- The first modes to become unstable will be of the form

$$a(\mathbf{r}, \phi) = \sum z_i e^{i\mathbf{k}_i \cdot \mathbf{r}} u(\phi - \varphi_i) + c.c$$

where  $\mathbf{k}_i = q_c(\cos \varphi_i, \sin \varphi_i)$  and the sum is over all wave vectors of this form.

- As indicated in (ii) above, the space of eigenfunctions decomposes into odd and even subspaces. To a first approximation the even modes have  $u(\phi) = \cos 2\phi$  and the odd modes have  $u(\phi) = \sin 2\phi$ .
- In the generic case the odd eigenmodes are excited before the even modes. However, under certain special conditions it is possible for even modes to be excited first. Even modes correspond to scalar contour patterns, and odd modes correspond to pseudoscalar contour patterns.
- The  $p = 0$  case is important because it corresponds to contourless scalar patterns, i.e. patterns of light and dark rather than a lattice of contours.

Lattice	Eigenfunctions
Square	$z_1 u(\phi) e^{ix} + z_2 u(\phi - \frac{\pi}{2}) e^{iy} + c.c$
Hexagonal	$z_1 u(\phi) e^{\mathbf{k}_1 \cdot \mathbf{r}} + z_2 u(\phi - \frac{2\pi}{3}) e^{\mathbf{k}_2 \cdot \mathbf{r}} + z_3 u(\phi - \frac{4\pi}{3}) e^{\mathbf{k}_3 \cdot \mathbf{r}} + c.c.$

Table 4: Eigenfunctions corresponding the shortest dual wave vectors for the square and hexagonal lattices.

#### 4.4 Restriction to a lattice

We now restrict the solutions to be doubly periodic on a lattice, choosing the size of the lattice so that the shortest dual wave vectors have size  $q_c$ . The symmetry group of the problem is thus reduced from  $E(2)$  to  $\Gamma = D_{2m} \rtimes T^2$ , where  $m = 2$  for a square lattice and  $m = 3$  for a hexagonal lattice.

We mentioned previously that there is no rigorous justification for the restriction to a lattice in general. In the case of the visual cortex though, we know that V1 is made up of a lattice of hypercolumns, which we approximated by a continuum. Thus we might like to think of the restriction to a lattice as modelling the lattice of hypercolumns. Indeed, many observed patterns are seen to have a wavelength in V1 which corresponds roughly to the spacing between hypercolumns.

The eigenfunctions for the square and hexagonal lattices are shown in Table 4. Thus we can identify the space of unstable eigenfunctions with the complex vector space spanned by the vectors  $(z_1, \dots, z_m) \in \mathbb{C}^m$ , with  $m = 2$  for the square lattice and  $m = 3$  for the hexagonal lattice. We can then follow the procedure in Section 3 to find the action of  $\Gamma$  on the space of unstable eigenfunctions in order to find the axial subgroups and classify the possible patterns. There are axial subgroups corresponding to both scalar and pseudoscalar patterns, which are very similar to the subgroups we found when we looked at patterns on the square and hexagonal lattices in Section 3.

Recall that when we linearized the Wilson-Cowan equation we discovered that there were three possible forms for  $u(\phi)$  depending on whether we were in the  $p = 1$  or  $p = 0$  cases:

- (i) Even contoured patterns with  $u(\phi) \approx \cos 2\phi$
- (ii) Odd contoured patterns with  $u(\phi) \approx \sin 2\phi$
- (iii) Even non-contoured patterns with  $u(\phi) \approx 1$ .

Pattern	Eigenfunction
Rolls	$u(\phi) \cos x$
Squares	$u(\phi) \cos x + u(\phi - \frac{\pi}{2}) \cos y$
Hexagons	$u(\phi) \cos \mathbf{k}_1 \cdot \mathbf{x} + u(\phi - \frac{2\pi}{3}) \cos \mathbf{k}_2 \cdot \mathbf{x} + u(\phi - \frac{4\pi}{3}) \cos \mathbf{k}_3 \cdot \mathbf{x}$

Table 5: Eigenfunctions with axial subgroups for the scalar case  $u(-\phi) = u(\phi)$ .

Pattern	Eigenfunction
Anti-rolls	$u(\phi) \cos x$
Anti-squares	$u(\phi) \cos x + u(\phi - \frac{\pi}{2}) \cos y$
Anti-hexagons	$u(\phi) \cos \mathbf{k}_1 \cdot \mathbf{x} + u(\phi - \frac{2\pi}{3}) \cos \mathbf{k}_2 \cdot \mathbf{x} + u(\phi - \frac{4\pi}{3}) \cos \mathbf{k}_3 \cdot \mathbf{x}$
Anti-triangles	$u(\phi) \sin \mathbf{k}_1 \cdot \mathbf{x} + u(\phi - \frac{2\pi}{3}) \sin \mathbf{k}_2 \cdot \mathbf{x} + u(\phi - \frac{4\pi}{3}) \sin \mathbf{k}_3 \cdot \mathbf{x}$
Anti-rectangles	$u(\phi - \frac{2\pi}{3}) \cos \mathbf{k}_2 \cdot \mathbf{x} - u(\phi - \frac{4\pi}{3}) \cos \mathbf{k}_3 \cdot \mathbf{x}$

Table 6: Eigenfunctions with axial subgroups for the pseudoscalar case  $u(-\phi) = -u(\phi)$ .

The even and odd patterns are summarised in Tables 5 and 6. Each pattern is approximately a steady-state solution of the modified Wilson-Cowan equation (30). All that remains is to determine how these patterns of neural activity in V1 correspond to hallucinations in the visual field. To do this we first need to interpret the patterns in a bounded domain in  $\mathbb{R}^2$ , which represents V1, and then we can use the inverse of the retino-cortical map described in section 4.1.

The simplest patterns to interpret are the non-contoured patterns, with  $p = 0$  and  $u \approx 1$ . There is no  $\phi$  dependence, and so we can treat the activity variable  $a(\mathbf{r}, \phi)$  as a simple scalar  $a(\mathbf{r})$  and colour code the pattern as, say, black for  $a(\mathbf{r}) > 0$  and white for  $a(\mathbf{r}) < 0$ .

The contoured patterns are trickier to interpret. At a given location  $\mathbf{r}$  we have a sum of sinusoidal functions, all with different phases and amplitudes. However, because we are in the  $p = 1$  case we know that the sum must be unimodal in  $\phi$ -space, so there is a value of  $\phi$  for which the amplitude is maximal. We interpret this to mean that the visual cortex has detected a contour at  $\mathbf{r}$  in the direction  $\phi$ , and we plot a local tangent in the direction  $\phi$  at  $\mathbf{r}$ .

## 4.5 Visual hallucinations

Now that we have an interpretation of the patterns in V1 we can attempt to put them into visual field coordinates to see how well they correspond to Klüver's form constants. For the non-contoured patterns we can simply use the inverse of the retino-cortical map described in section 4.1. However, we hit a problem when we try to map contoured patterns to the visual field: we have no way of mapping the orientations. The mapping described in Section 4.1 was for a scalar field, i.e. a pattern of light and dark patches, and with a contoured pattern we essentially have a vector field. If  $\phi$  represents an orientation in V1, we want to find the appropriate orientation  $\phi_R$  in the visual field.

We solve this problem by thinking about tangents to oblique lines in V1, and the corresponding tangents to logarithmic spirals in the visual field. A line in V1 with slope  $y/x = \tan \phi$  is a level curve of the equation

$$f(x, y) = y \cos \phi - x \sin \phi$$

where  $(x, y)$  are Cartesian coordinates in V1. If we think of  $\{\partial/\partial x, \partial/\partial y\}$  as a basis for the tangent

space of V1, then such a line has a constant tangent vector

$$\mathbf{v} = \cos \phi \frac{\partial}{\partial x} + \sin \phi \frac{\partial}{\partial y}.$$

If we now change from cortical coordinates to visual field coordinates using the transformation given in (29), we find that the preimage in the visual field of such a line is

$$g(r, \theta) = \theta \cos \phi - \log r \sin \phi$$

and that the level curves of the function are logarithmic spirals,

$$r = A \exp(\theta \cot \phi).$$

We can then calculate the 1-form  $dg$ , and find the tangent vector  $\tilde{\mathbf{v}}$  to the spiral by demanding that  $\langle dg | \tilde{\mathbf{v}} \rangle = 0$ . We find that

$$\tilde{\mathbf{v}} = r \cos \phi \frac{\partial}{\partial r} + \sin \phi \frac{\partial}{\partial \theta}.$$

We can then convert into Cartesian coordinates  $(x_R, y_R)$  in the visual field, using  $x_R = r \cos \theta$  and  $y_R = r \sin \theta$ . This gives

$$\tilde{\mathbf{v}} = r \cos(\phi + \theta) \frac{\partial}{\partial x_R} + r \sin(\phi + \theta) \frac{\partial}{\partial y_R}.$$

Thus the retinal vector field induced by a constant vector field in V1 ‘twists’ with the polar angle  $\theta$ , and stretches with the radius  $r$ . By comparison with the expression for  $\mathbf{v}$  above, we see that if  $\phi_R$  is the orientation of a contour in the visual field then we must have  $\phi_R = \phi + \theta$ . Thus the inverse map from V1 coordinates to visual field coordinates is given by

$$r = \frac{1}{\epsilon} \exp(\alpha x / \epsilon), \quad \theta = \frac{\epsilon y}{\beta}, \quad \phi_R = \phi + \theta.$$

Using this we can see what the patterns of neural activity in V1 look like when viewed in visual field coordinates. Some results are shown in Figure 9.

Note that one thing we have not done so far is explicitly calculated the amplitude equations and analysed the stabilities of patterns, to determine which patterns are most likely to be selected. This

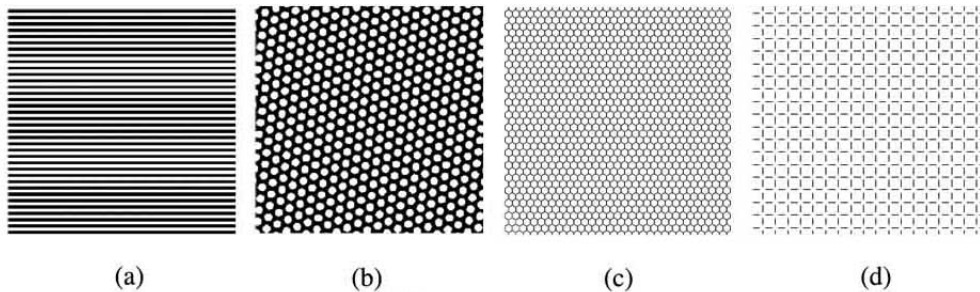


Figure 8: V1 patterns corresponding to some axial subgroups: (a) scalar rolls, (b) scalar hexagons, (c) even hexagons and (d) even squares.

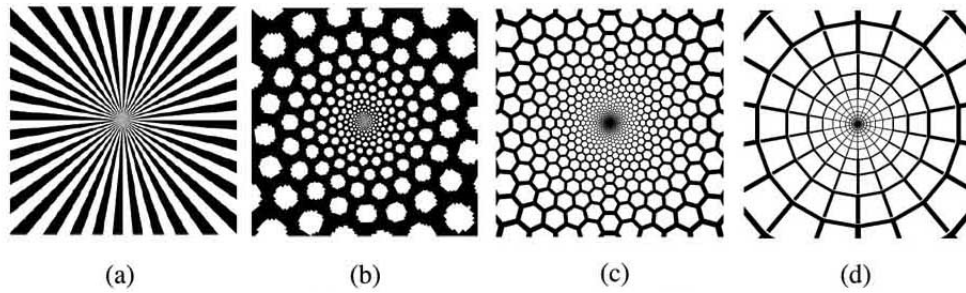


Figure 9: The same patterns as in Figure 8 now drawn in visual field coordinates. We clearly recognise the four Klüver form constants: (a) funnel, (b) spiral, (c) honeycomb and (d) cobweb.

is relatively easy to do, but it is not particularly exciting. Suffice to say that in Figure 8 I have chosen to show the stable patterns and omit the unstable ones. It is fortuitous that these are the patterns which correspond to the most commonly observed form constants.

What does this tell us about the architecture of the primary visual cortex? Firstly, the predictions of the model lend weight to the theory of intricate anisotropic neural couplings in V1. Secondly, the model predicts that the mechanism by which visual hallucinations are generated is closely related to the mechanisms for processing edges and contours. Further study of the novel ‘shift-twist’ representation of the Euclidean group could prove important for producing algorithms to enable computers to effectively detect edges and contours, which has thus far been a major problem in pattern-recognition problems such as automated face recognition.

## References

- [1] M. Golubitsky, I. Stewart and D. Schaeffer. *Singularities and Groups in Bifurcation Theory II*, 1988.
- [2] M. Golubitsky and I. Stewart. *The Symmetry Perspective: From Equilibrium to Chaos in Phase Space and Physical Space*, 2000.
- [3] R. Hoyle. *Pattern Formation: An Introduction to Methods*, 2006.
- [4] M. Golubitsky and B. Dionne. *Planforms in two and three dimensions*, 1992.
- [5] I. Bosch Vivancos, P. Chossat and I. Melbourne. *New planforms in systems of partial differential equations with Euclidean symmetry*, 1995.
- [6] A. Huxley. *The Doors of Perception*, 1954.
- [7] G. Ermentrout and J. Cowan. *A mathematical theory of visual hallucination patterns*, 1979.
- [8] P. Bressloff, J. Cowan, M. Golubitsky, P. Thomas and M. Wiener. *Geometric visual hallucinations, Euclidean symmetry, and the functional architecture of the striate cortex*, 2001.
- [9] P. Bressloff, J. Cowan, M. Golubitsky, P. Thomas and M. Wiener. *What geometric visual hallucinations tell us about the visual cortex*, 2002.